IEEE Access
Multidisciplinary | Rapid Review | Open Access Journal

Received June 20, 2020, accepted June 30, 2020, date of publication July 3, 2020, date of current version August 3, 2020.

*Digital Object Identifier 10.1109/ACCESS.2020.3006868*

# Architecture of Cloud 3D Printing Task Modeling for Nodes Dynamic Scheduling and Coupling Based on Complex Networks

**CHENGLEI ZHANG[1,2,3], JIAJIA LIU[1,3], BO XU[1], BO YUAB[4], SHENLE ZHUANG[2], AND FEIYU ZHAO[5]**

[1]School of Mechanical and Vehicle Engineering, Linyi University, Linyi 276000, China
[2]Shandong Longli Electronic Company Ltd., Linyi 276000, China
[3]Linyi Institute of Intelligent Manufacturing and Design, Linyi 276000, China
[4]School of Mechanical and Electrical Engineering, Wuhan City Polytechnic, Wuhan 430064, China
[5]School of Computer Science, South-Central Minzu University, Wuhan 437006, China

Corresponding author: Chenglei Zhang (zhangchenglei@lyu.edu.cn)

This work was supported in part by the Natural Science Foundation of Shandong Province of China under Grant ZR2019PEE019; and in part by the High-level talents (high-level doctorate) research project of Linyi University under Grant LYDX2019BS009.

**ABSTRACT** To study the variation in resource allocation efficiency in a cloud 3D printing (C3DP) manufacturing grid, C3DP task modeling for a complex network model was established based on the dynamic coupling of nodes, taking cloud manufacturing resource characteristics such as distribution and diversity into account. Based on this idea, we propose an architecture of C3DP task modeling for complex networks based on the dynamic coupling of nodes. First, the model calculates the initial tasks and services by evaluating the quality of the manufacturing resources, and then, according to the strength of the correlations among various tasks and among services and tasks, a multiplex network model based on cloud tasks and services is constructed. Then, according to the description and its constraint structure definition of the C3DP order tasks, by using the intercept method for complex networks, this paper identifies the work breakdown structure of coupling task sets, simplifies the optimization process, and proposes a C3DP order task (C3DPOT) network modeling method. Third, on the basis of the formal description of C3DP service resources, an architecture of C3DP order task methods for complex networks based on the dynamic coupling of nodes is proposed. Finally, a Service_Net model example is designed to verify the feasibility of the method.

**INDEX TERMS** Complex networks, manufacturing resource services, service-oriented manufacturing (SOM), cloud 3D printing, work breakdown structure, dynamic coupling of nodes.

## ABBREVIATIONS

| | |
|---|---|
| C3DP | Cloud 3D printing |
| C3DPS | Cloud 3D printing Services |
| C3DPOT | C3DP order task |
| MFG | Manufacturing |
| AMSs | Advanced MFG modes and systems |
| CMfg | Cloud MFG |
| MSO | Small batch and older |
| HPI | Hub promoted index |
| CN | Common Neighbors |
| PA | Preferential Attachment |
| AA | Adamic-Adar |
| RA | Resource Allocation |
| CI | Combining Index |
| NS | Net Science |
| PB | Political Blogs |

The associate editor coordinating the review of this manuscript and approving it for publication was Yilun Shang.

## I. INTRODUCTION

Manufacturing (MFG) is undergoing rapid changes, along with the rapid development of information technology and other related technologies. Numerous demand-driven and technology-driven factors have prompted current MFG to become agile, networked, service-oriented, green, sustainable and social [1]. To enable the MFG industry and its corresponding MFG enterprises to adapt to these changes, and to support the improvement of the informatization degree, innovative product design and production, and the efficient use of resources, a number of

advanced MFG modes and systems (AMSs) have been proposed in recent years [2]. These include flexible MFG, computer-integrated MFG, agile MFG, sustainable MFG, networked MFG, service-oriented MFG, and cloud MFG(CMfg) [5]. In particular, when the quantity of customer orders is large or urgent, these service providers' resources and capabilities cannot meet the needs of customers. Aiming at achieving creative innovation design and product customization, a multiple-variety, small batch and older (MSO) model with a market orientation is proposed [6], [43]. At the same time, 3D printing service providers have used the Internet to connect users who form various links in the industrial chain [7]. Customer requirements are integrated into large orders and then decomposed into small tasks, or decentralized design resources (such as Maker) are integrated into cloud design and design tasks are assigned.

Cloud 3D printing services (C3DPSs) involve many industries, types of knowledge and data scales, and there are problems with understanding ambiguity and nonstandard terminology in natural language descriptions [9]. At present, the format of the exchange between these services' and the order tasks' information in cloud 3D printing (C3DP) is not uniform, which affects the efficient processing of order tasks and service matching in C3DPS platforms [8]. To address the ambiguity in the services' and order tasks' information, complex and heterogeneous resources are required along with unified descriptions and modeling. The process of executing a C3DP order task (C3DPOT) can be regarded as performing a series of C3DPSs that are combined according to a certain schedule and logical relationship to complete the corresponding MFG task activity. It is an organic collection of the services' and tasks' active objects (such as the order type, processing steps, delivery time, and product material) based on time, information, and physical flow. The architecture of C3DP tasks and services is the basis for information monitoring and processing in the process of executing order-driven C3DP tasks [11]. This order task and service model can formally represent the information of such tasks and effectively integrate and manage the data of services and MFG tasks. Additionally, the information description in each stage of the C3DPOT execution process is not only a formal semantic description of the equipment resources needed but also a potential source of sensitive information such as semantic descriptions and knowledge discovery, matching and combination. The use of an online store, reasoning, queries, and access to the knowledge and information of the formally defined task knowledge and data of a C3DPS order is the basis for constructing the C3DPS platform.

CMfg is based on the concept of ''manufacturing as a service'' and is a new concept originating from cloud computing [12]. The enabling technologies of CMfg include task allocation, trust evaluation technology, and personalized knowledge service technology. At present, scholars around the world mainly focus on the static matching problem of CMfg supply and demand for quantitative research. The static matching of supply and demand mainly includes the selection of CMfg services and the scheduling of MFG tasks [13]. However, a 3D printing service provider operates in a market-driven order production mode, and dynamic demand has always been dominant in production.

C3DP is based on the emerging cloud manufacturing services of ''manufacturing on demand'' and ''manufacturing as a service''. It applies to the additive manufacturing industry, which has achieved the rapid response of printing services and the efficient and energy-saving use of printing resources and is progressing toward better networked printing [3]. Therefore, a C3DP business involves the integration of 3D printer equipment resources based on the Internet, the construction of roaming and shared printing platforms, and a superior form of networked printing. Therefore, a C3DP business uses quality-standardized printing services in a roaming and shared printing platform that has been integrated with 3D printing equipment resources based on the Internet, which an entire society can use at any time and place [14].

There are few studies on supply dynamics, and they have mainly focused on describing uncertainties in supply and demand and on building different types of global dynamic service matching models and optimization algorithms for dynamic service matching resources [4]. Because C3DPS supply and demand matching is a dynamic service matching method of multistage services, the dynamic matching problem of supply and demand cannot address actual dynamic demand.

C3DP order tasks are part of the on-demand work flow process of task allocation in the CMfg mode; that is, they meet the needs of a certain C3DPS so that customers can publish printing tasks to the cloud platform of a cloud service provider through various terminals (e.g., 3D scanning, 3D design, calculation simulation, quotation calculation, slice processing, 3D printing, surface processing, warehousing services, and logistics distribution) [8]. Here, the requirements of the C3DP order task are reflected in the heterogeneity of different DD workshops and different order tasks. In short, C3DP order tasks enable distributed customers to customize printing services in the C3DPS platform. The system makes a judgment according to the region and the nature of the order and decomposes a large order into multiple offline DD printing workshops to perform granular tasks. At the same time, the cloud collaboration of the C3DP task scheduling is dispatched to the best printer [8].

Therefore, considering the aforementioned characteristics, to ensure the quality and efficiency of MFG services in cloud environments, the main contribution of this work is a descriptive model of C3DPSs, which easily matches the demand for MFG tasks directly on the demand side, thereby achieving service transactions [15]. However, the probability of these services being invoked individually is small,

especially considering the personalized design requirements of innovative and creative products over the whole product life cycle. Based on this idea, the best group of services is usually selected and combined with other services [16]. Considering that the MFG service description model in the traditional cloud MFG service portfolio can only be matched with MFG task requirements, a C3DPS network is proposed that can create a self-organizing cluster among C3DPS resources.

To handle the dynamic characteristics of C3DPOTs, we propose a C3DP task modeling method based on order-driven considerations. In this modeling method, a multiplex network model based on C3DP task services (T_S_Network) is proposed, which includes an order task network ($T\_Net$) and a service network ($S\_Net$). It consists of multiple associations among services and services, tasks and tasks, and services and tasks. In the C3DPOT network modeling process, order task-related semantic information can be expressed by the domain ontology modeling method. Additionally, it can be better to reuse the semantic description and semantic knowledge. Finally, an example is given to verify the feasibility of the multiplex C3DP task network model.

## II. MODELING OF A MULTIPLEX NETWORK BASED ON C3DP TASK SERVICES

### A. THE DYNAMIC SCHEDULING CHARACTERISTICS OF THE TASK-SERVICE NETWORK

A task-service network refers to a model that includes a MFG network and MFG task network model based on a complex network in a C3DP environment, according to a digital description of the services and tasks [17]. A task-service network is a network derived from the theory of complex networks and C3DP, so it has the following characteristics:

#### 1) RELEVANCE

When the users' order tasks have been submitted to this platform, they are decomposed into a certain number of granular atomic tasks through the service demand decomposition module. For example, a certain type of artistic sculpture MFG task can be decomposed into six tasks-conceptual design tasks, three-dimensional modeling tasks, simulation calculation tasks, 3D printing tasks, post-processing tasks, and logistics tasks—according to different conditions and constraints [21]. These tasks and services use semantic information and domain knowledge. There is a relationship between tasks and services, and the decomposed atomic tasks inherit the basic task information of the parent task [18]. Therefore, the task-service nodes are also associated with the task-service network.

#### 2) MULTIPLE COMPLEXITY

The task-service network includes a $T\_Net$ and an $S\_Net$. The $T\_Net$ is composed of several subtask networks $(G_1, G_2, G_3, \ldots, G_m)$. In the task-service network, nodes can represent anything; there are great differences in the content, constraints, quality requirements and connection weights among nodes [19]. For example, the task network is composed of several single atomic tasks according to order task relationships, and a service network node represents a single resource for C3DPSs based on a complex network. Therefore, a task-service network has a large number of nodes and various node types; this network structure also exhibits the complexity of multiple networks.

#### 3) NODE CLUSTERING

A task-service network also tends to exhibit clustering. For example, the C3DPS selection set contains candidate basic services that can complete atomic tasks $t_p$. Each candidate basic set is composed of several of the same types of services [20].

#### 4) UNIQUENESS

A newly added node can be described accurately and does not conflict with the existing nodes in the task-service network. In the description process for the dynamic coupling of nodes, it is necessary to ensure that the semantic descriptions of similar nodes are unique and that there is only one description of each node.

### B. THE WORK BREAKDOWN STRUCTURE IN THE MULTIPLEX NETWORK MODEL

The working principle of a C3DP task service network is to aggregate tasks in atomic task sequences, which means that data is mapped to resources and order tasks of different granularities, and an optimal service composition scheme for candidate C3DPS sets is generated [22]. Fig. 1 shows a diagram of the customized enterprise order conversion process.

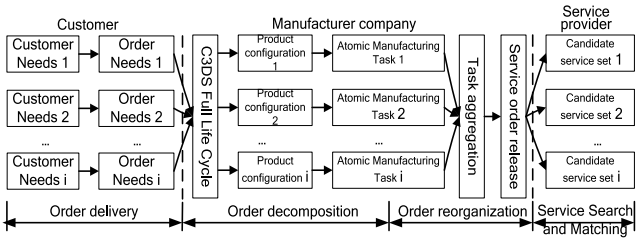


**FIGURE 1. Diagram of the customized enterprise order conversion process.**

Based on this fact, the work breakdown structures in the aggregation and optimization of C3DPOTs are mathematically described as follows:

#### 1) TASK DECOMPOSITION AND EXPRESSION

The submitted MFG task is decomposed into a number of atomic tasks $t_p$ with a certain granularity through the service demand decomposition module by the service demand side to yield a set of atomic tasks $p = (1, 2, \ldots, c)$, where $c$ is the

number of atomic tasks.

$$T = \{t_1, t_2, \ldots, t_i, \ldots, t_p\} \tag{1}$$

It can also be decomposed into several fine-grained MFG tasks $t_p^j$ according to its task type, which can be expressed as:

$$t_p = \{t_p^1, t_p^2, \ldots, t_p^j, \ldots, t_p^n\}, \tag{2}$$

where $t_p^j$ represents the j-th MFG task of $t_p$, which is decomposed according to the task type, where $j = (1, 2, \ldots, n)$ and $n$is the number of MFG task types [23]. Fig. 2 shows a diagram of the C3DP order atomic task sequence.

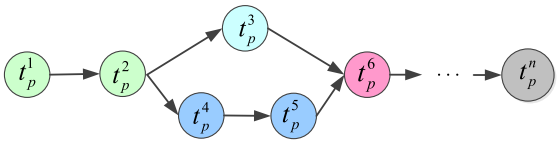

**FIGURE 2.** Diagram of the C3DP order atomic task sequence.

### 2) DESCRIPTION OF THE CANDIDATE SERVICE SEQUENCE

The C3DPOT sequence set $A$ is composed of several services in the C3DPOT platform, namely:

$$A = \begin{bmatrix} 0 & t_{12} & \cdots & t_{1N-1} & t_{1N} \\ t_{21} & 0 & \cdots & t_{2N-1} & t_{2N} \\ \vdots & \vdots & \ddots & \vdots & \vdots \\ t_{N-11} & t_{N-12} & \cdots & 0 & t_{N-1N} \\ t_{N1} & t_{N2} & \cdots & t_{NN-1} & 0 \end{bmatrix}, \tag{3}$$

where $A$ is a directed graph that can be represented by a matrix that flows from the first node to the N-th node, as shown.

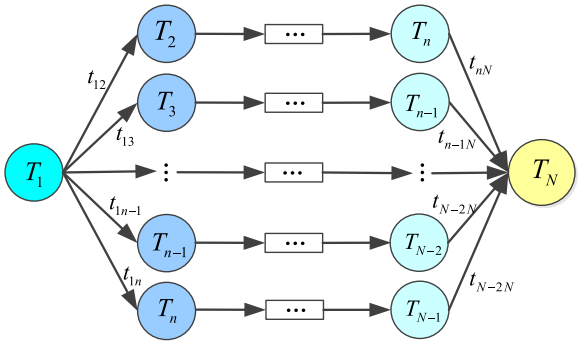

**FIGURE 3.** Diagram of the C3DPS sequence.

For an atomic task sequence, the corresponding candidate C3DPS sequence is generated as follows:

$$t_{ij} \rightarrow WS_{ij} = \{WS_{p_1}^j, WS_{p_2}^j, \ldots, WS_{p_m}^j\}, \tag{4}$$

where $WS_p^j$ is a candidate C3DPS set for atomic tasks. Fig. 3 shows a diagram of the C3DPS sequence.

From the above formulas, the relationship between the atomic tasks is generated by the order demand decomposition and the corresponding candidate C3DPS sets [13]. The dynamic coupling of the nodes in the C3DPS portfolio is shown in Fig. 4.

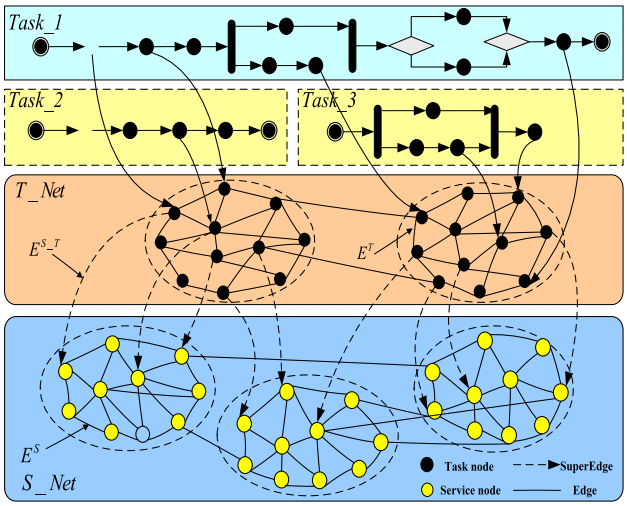


**FIGURE 4.** Diagram of the dynamic coupling of the nodes in the C3DPS portfolio.

A candidate C3DPS set can perform many kinds of MFG tasks.

From the above information, we can see that a C3DPS portfolio matrix can be expressed as:

$$M = \begin{array}{c} \\ t_{1P_1} \\ \vdots \\ t_{nP_n} \end{array} \begin{array}{c} \begin{array}{ccc} WS_{p_1}^1 & \cdots & WS_{p_n}^m \end{array} \\ \begin{bmatrix} WS_{p_1}^1 & \cdots & WS_{p_1}^m \\ \cdots & \ddots & \cdots \\ WS_{p_n}^1 & \cdots & WS_{p_n}^m \end{bmatrix} \end{array}, \tag{5}$$

### 3) THE TASK-SERVICE NETWORK MODEL

There are two types of nodes and three types of edges in the task-service network model for C3DP. Specifically, the two types of nodes are expressed as follows:

1. Service nodes are abstracted from various resources and capabilities in C3DP MFG and are represented as service nodes in the *S_Net*;
2. In the C3DPS public platform, a task node can perform an order task in real-time operation in the *T_Net*, and it is represented as:

*Definition 1 (Superedge):* Assume *T_Net* is a finite set. Then

$$1) \quad e_i \neq \Phi (i = 1, 2, \ldots, m), \tag{6}$$

$$2) \quad \bigcup_{i=1}^{m} e_i = V, \tag{7}$$

where $H = (V, E)$ refers to the binary relation of a hypergraph [25];

$v_1, v_2, \ldots, v_n$ refers to nodes in the hypergraph that are elements of $V$;

$e_i = \{e_i^1, e_i^2, \ldots, e_i^j\}$ $(i = 1, 2, \ldots, m; j = 1, 2, \ldots, n)$ is called the edge of the hypergraph or the hypergraph edge.

In addition, these correlations are constructed as hypergraph edges in the networks *S_Net* and *T_Net*. Therefore, the three types of edges are expressed as follows:

a. The edges of service nodes in *S_Net* can be represented as $E^S$;
b. The edges of task nodes in *T_Net* can be represented as $E^T$;
c. The edges of service and task nodes in *S_Net* and *T_Net* can be represented as $E^{S\_T}$.

For these service requirements, the key principle is to match a candidate C3DPS set and the atomic task in the business process of all sequences, and the best service is then selected from the candidate C3DPS set in the C3DPS portfolio [12], [27]. Based on the relationships among these nodes, a multiplex network based on C3DP task services is formed. Fig. 5 shows the multiplex network based on C3DP task services.

$E^{S\_T}$ are the superedges (logical relationships) between task network nodes and service network nodes in the C3DP task-service network; $E^T$ is an edge between a C3DPOT node and a C3DPOT node; and $E^S$ is an edge between a C3DPS node and a C3DPS node [28], [29].

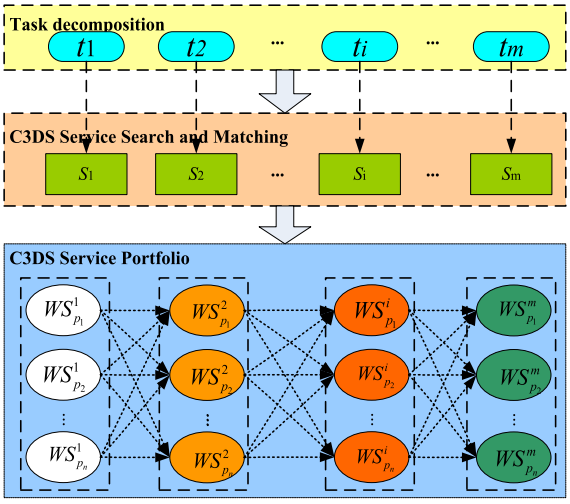


**FIGURE 5.** The multicomplex network based on C3DS task services.

## III. THE METHOD OF C3DPOT NETWORK MODELING

The digital description of a C3DPOT is supported by a unified semantic expression and by data for C3DPOT decomposition and C3DPS matching. Therefore, network modeling and description are key steps in the implementation of the C3DPS task execution process [30], [31]. However, there are some great differences between C3DPOT nodes and C3DPS nodes. In view of this, this paper proposes a method of C3DPOT network modeling in which a semistructured data process converts C3DPOT ontological semantic information into an Ontology Web Language for Services (OWL-S), and semistructured data are encapsulated with the modeling method of the C3DPOT network, that is, the semantic description of document nodes and link attributes [32].

### A. C3DPOT DESCRIPTION AND THE DEFINITION OF ITS CONSTRAINT STRUCTURE

Not only does the C3DPOT information model have dynamic characteristics, but it is also limited to basic task information. For this reason, this paper constructs a model of the C3DPOT description and gives C3DPOT information fragments based on OWL-S [33]. Fig. 5 and Fig. 6 show the model of the C3DPOT description and task information fragments. The information model can be described as a triple, as follows:

$$C3DS\_Task ::= \{Task\_Info, Subtask\_Set, Relation\_Set\}, \quad (8)$$

where *Task_Info* represents the total information of the C3DPOT; *Subtask_Set* represents the C3DPOT activity collection; and *Relation_Set* represents the C3DPOT activity relation set.

The described elements of the C3DPOT information are as follows:

#### 1) THE TOTAL INFORMATION OF THE C3DPOT

The total information of the C3DPOT is expressed in triple form as follows:

$$Task\_Info ::= \{Task\_StaticInfo, Task\_DynamicInfo, Task\_QoSReq\}, \quad (9)$$

where *Task_StaticInfo* represents the description of the C3DPOTs' static information;

*Task_DynamicInfo* represents the description of the C3DPOTs' dynamic information; *Task_QoSReq* represents the quality of service (QoS) requirements for C3DP order tasks.

1. Description of the C3DPOTs' static information (*Task_StaticInf*)

The main function of *Task_StaticInf* is described by the C3DPOTs' basic information [34], [35]. According to the characteristics of the C3DPOT, *Task_StaticInf* can be expressed as the following seven-tuple:

$$Task\_StaticInf ::= \{Task\_Id, Task\_Name, Task\_ContentTask\_Type, Task\_PropertyList, \quad (10)$$

where *Task_Id* is the ID of the C3DPOT;

*Task_Name* is the name of the C3DPOT;

*Task_Content* indicates the complete content of the C3DPOT;

*Task_Type* is the type of the C3DPOT, such as the design, integrated service, MFG, simulation, or logistics category [36];

*Task_PropertyList* represents a custom attribute set of the C3DPOT, which mainly includes the structure, behavior, and

function information of the C3DPOT, such as the task owner, the task number, and the task batch;

*Other* indicates other tasks' static information.

2. Description of the C3DPOTs' dynamic information (*Task_DynamicInfo*)

*Task_DynamicInfo* can be expressed as the following five-tuple:

$$Task\_DynamicInfo ::= \{Task\_Id, Task\_Schedule, Task\_Duration, Task\_Status, Other\}, \quad (11)$$

where *Task_Schedule* represents the execution progress information of the C3DPOT;

*Task_Duration* represents an execution time period of the C3DPOT;

*Task_Status* indicates the status information of the C3DPOT, such as normal, paused, or terminated;

*Other* indicates other task dynamic information.

3. The description of the C3DPOTs' QoS Request (*Task_QoSReq*)

*Task_QoSReq* mainly includes the time, cost, quality and other requirements for C3DPOT execution and can be represented as the following five-tuple:

$$Task\_QoSReq ::= \{Task\_Id, Task\_Time, Task\_Cost, Task\_Quality, Other\}, \quad (12)$$

where *Task_Time* indicates the time when the order task is executed;

*Task_Cost* indicates the C3DPOT execution cost;

*Task_Quality* indicates the C3DPOT execution quality;

*Other* indicates the other C3DPOTs' execution information.

#### 2) THE C3DPOT ACTIVITY COLLECTION (*Subtask_Set*)

*Subtask_Set* refers to a larger order task that is decomposed into several C3DP atomic tasks with different granularities according to the task type, activity object feature information and service constraints [37], [38]. The formal description of the C3DP order activity is as follows:

$$Subtask\_Set ::= \{ActQoSReq, ActFeature, ActServReq\}, \quad (13)$$

where *ActQoSReq* represents a subset of the activity service quality requirement information of the C3DP task, which is consistent with the description form of *Task_QoSReq*;

*ActQoSReq* represents the characteristics of an active object, which refers to the representation attributes, technical attributes, functional attributes, etc.;

*ActServReq* represents a collection that meets the activity requirements.

#### 3) THE C3DPOT ACTIVITY RELATIONSHIP SET (*Relation_Set*)

*Relation_Set* refers to the mapping set of logical sequential relationships between the task activities of a C3DP order, such as the serial connection, parallelism, selection, and coupling of various activities in the complex product collaborative development process [39].

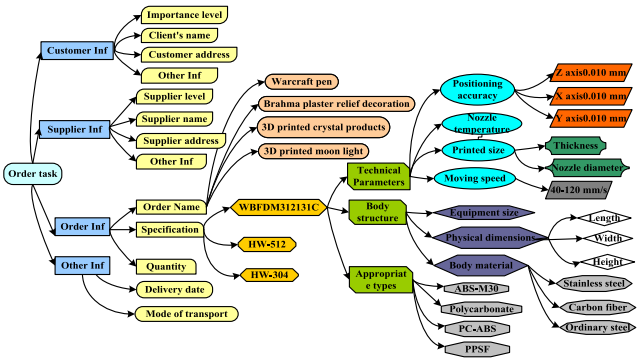


**FIGURE 6.** The knowledge ontology description model of the C3DP order task.

### B. THE PROCESS OF CONSTRUCTING A C3DPOT NETWORK

Taking a 3D portrait printing service as an example of constructing a C3DPOT network, the fashionable and customized 3D human portrait printing product is made of colored plastic, and the printing precision has certain requirements. Regarding the materials used, 3D human portrait printing products are currently made of gypsum, plastic, food materials and other materials. In the early stage of image printing products, the printing demand was divided into six subtasks: 3D modeling, portrait scanning, cartoon image design and modeling, 3D portrait printing, surface post-processing, and coloring [40]. Fig. 7 shows the 3D portrait printing task decomposition diagram.

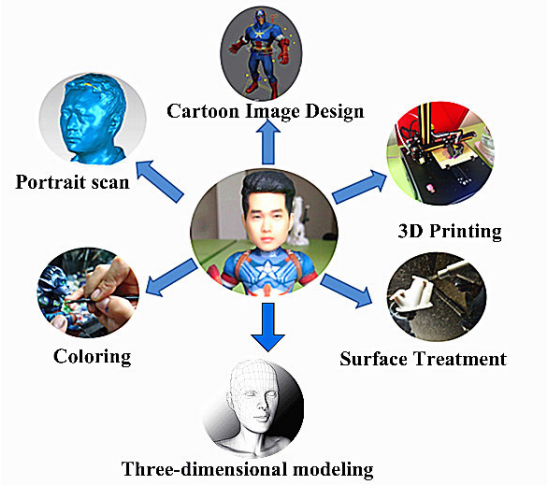


**FIGURE 7.** The 3D portrait printing task decomposition diagram.

In the C3DPOT network, the nodes and the connected edges represent the most basic principles. To simulate a complex order task network, the construction of the C3DP order model should be studied first. The main components are as follows:

### 1) THE SELECTION OF NODES

It is obvious that the order task units (such as portrait scanning, cartoon image design and modeling, model slicing, 3D portrait printing, surface post-processing, and coloring) in C3DP are nodes of the C3DPOT network. Although the types of order tasks in C3DP are different, the assumed roles are also quite different. Additionally, in the semantic description process of C3DP order tasks, all the task units are processed into task nodes [41].

In view of this, the selection process of nodes should be analyzed. The details are as follows:

First, the OWL-S order task unit data in the network are abstracted into nodes with directed graphs and transformed into an nth-order matrix.

Assuming that the distance of the source node SID is $ds$, the expression of the nth-order matrix A is:

$$A = \begin{bmatrix} 0 & 1 & 0 & 0 & 1 & 0 & 0 & 0 & 0 \\ 1 & 0 & 1 & 1 & 1 & 0 & 0 & 0 & 0 \\ 0 & 1 & 0 & 1 & 1 & 1 & 1 & 1 & 1 \\ 0 & 1 & 1 & 0 & 1 & 0 & 0 & 0 & 0 \\ 1 & 1 & 1 & 1 & 0 & 0 & 0 & 0 & 0 \\ 0 & 0 & 1 & 0 & 0 & 0 & 1 & 1 & 0 \\ 0 & 0 & 1 & 0 & 0 & 1 & 0 & 1 & 0 \\ 0 & 0 & 1 & 0 & 0 & 1 & 1 & 0 & 1 \\ 0 & 0 & 1 & 0 & 0 & 0 & 0 & 1 & 0 \end{bmatrix}, \quad (14)$$

where $a_{ij}$ indicates whether there is a join between two nodes. If the edge is not connected, the corresponding matrix element is 0; otherwise, it is 1.

Second, we calculate the proper vector weight.

If the weight of a proper word is$f_t$, the weight of each characteristic word's proper vector in the unit data $W_i$ is calculated as follows:

$$W_i = \sigma \times \mu \times f_t \times \log(l + 1), \quad (15)$$

where $\sigma$ is the weighting coefficient of the location of the characteristic words; $\mu$ is the weighting coefficient of semantic analysis; $f_t$ is the frequency of each keyword in the order task unit data; and $l$is the distance between the key characteristic words.

Third, the pair sets and concepts in the nodes are constructed.

According to the constraints, a pair's sets and concepts among the must-link nodes are compared to the pair's sets and concepts among the cannot-link nodes. On this basis, it is also determined whether the must-link nodes satisfy the above extended conditions, and the extent of prior knowledge is calculated.

The constraint of must-link nodes $C_{ml}$, $\forall V_i, V_j \in V, (V_i, V_j) \in C_{ml}$, indicates that node $V_i$and node $V_j$belong to the same type of network nodes. The intermediate values between the nodes that meet this constraint are recorded as 0.

The constraint of cannot-link nodes $C_{cl}$, $\forall V_i, V_j \in V$, $(V_i, V_j) \in C_{cl}$, indicates that node $V_i$ and node $V_j$ do not belong to the same type of network nodes. The intermediate values between the nodes that meet this constraint are recorded as $+\infty$.

According to these constraint rules, all C3DPOT unit data concepts $C = (C_1, C_2, \ldots, C_n)$ can be constructed. Here, they are selected and calculated from the important concepts $C_i$, and the expression is as follows:

$$\cup C_{i.}g = C_i \cup C_{i.}m = M, \quad (16)$$

where $M$ is the set of concepts; $C_i$ is the i-th concept of $C = (C_1, C_2, \ldots, C_n)$; $C_{i.}g$ is an object in $C_i$; $C_{i.}m$ is the attribute to which the concept set of C3DPOT unit data belongs; $g$ represents the object concepts; and $G$ represents the set of object concepts.

If $C(g, m)C_{i.}g = \emptyset$ and $C_{i.}m = \emptyset$, then

a. If $C_{i.}g + Cg < G$ and $C_{i.}m + C_{.}m < M$,then $C_{.}g = C_{.}g + C_{i.}g$ and $C_{.}m = C_{i.}m + C_{.}m$;
b. If $C_{i.}g + C_{.}g < G$ or $C_{i.}m + C_{.}m < M$, then the nodes are calculated by cycle and extracted from the set of all concepts.

Therefore, the features of all concepts are charted and normalized in the C3DPOT unit data, and these data are sequentially abstracted into a directed graph. The normalized calculation formula is as follows:

$$\bar{C}_i = \frac{C_i}{||C_i||} = \frac{C_i}{\left[(C_i^1)^2 + (C_i^2)^2 + \ldots + (C_i^m)^2\right]^{1/2}} \quad (17)$$

where $C_i$ is the i-th concept and $C_i^m$ is the first concept with a sememe, which is the smallest unit of meaning used to describe a concept. For example, attributes can be expressed as ''attributes'', entities can also be called ''entities'', etc.

Finally, the distance measurement between node pairs is calculated.

X is the first concept, and X is the i-th concept with a sememe.

Finally, the distance metric between pairs of nodes is calculated.

The distance measurement according to the smoothing hypothesis between concepts is calculated as follows:

$$d_{c_i,c_j} = ||\bar{C}_i - \bar{C}_j||_A = \sqrt{(\bar{C}_i - \bar{C}_j)^T A(\bar{C}_i - \bar{C}_j)}, \quad (18)$$

where $C_i$ is any concept with unit data in the C3DPOT; $d_{c_i,c_j}$is a smoothing hypothesis distance between $C_i$ and $C_j$.

### 2) THE FORMATION OF THE HYPERGRAPH EDGE

In the C3DPOT network, the edges of each node are determined by the existence of a timing constraint relationship between MFG tasks. Similarly, the edges in the C3DPOT network represent the logical structure and dependencies between nodes [42]. In a real network, there is not only one edge between two nodes, which allows one node to be associated with several nodes and then indirectly connected to achieve information exchange between nodes.

*Definition 2 (Adjacency Matrix):* $A_n = [a_{ij}]$ refers to the matrix that describes the adjacency relationship of abstract

**TABLE 1.** Boolean design framework matrix based on the 3D portrait printing order MFG task.

| | $t_1$ | $t_2$ | $t_3$ | $t_4$ | $t_5$ | $t_6$ |
|---|---|---|---|---|---|---|
| $t_1$ | **1** | 1 | 1 | 0 | 0 | 0 |
| $t_2$ | 0 | **1** | 0 | 0 | 1 | 0 |
| $t_3$ | 0 | 0 | **1** | 0 | 1 | 0 |
| $t_4$ | 0 | 0 | 0 | **1** | 0 | 1 |
| $t_5$ | 0 | 0 | 0 | 0 | **1** | 1 |
| $t_6$ | 0 | 0 | 0 | 0 | 0 | **1** |

business processes.

$$a_{ij} = \begin{cases} 1 & i \text{ and } j \text{ are } adjoined \\ 0 & i \text{ and } j \text{ are } no\text{-}adjoined, \end{cases} \tag{19}$$

where $a_{ij}$ represents a path between nodes. If $a_{ij} = 1$, then there is a path between the corresponding nodes; $a_{ij} = 0$ means that the nodes are not connected.

Therefore, the adjacency matrix of the C3DPOT network is described to determine whether there are associations between the tasks in the 3D portrait printing task, and it is transformed into a 6th-order Boolean design framework matrix. An example diagram is shown in Table 1.

Fig. 8 shows the abstracted business process diagram. The diagram is composed of a set of vertices and a set of edges that represent the 6th-order task vertices in a two-dimensional array, and the adjacency matrix is expressed as:

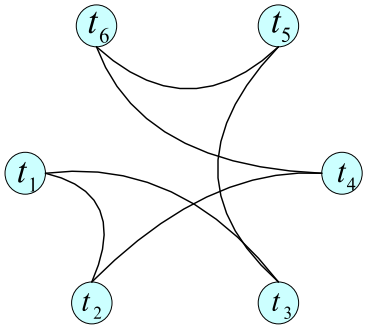


**FIGURE 8.** The abstracted business process diagram.

According to this adjacency matrix, a *T_Net* model is constructed for the 6th-order task vertices in a two-dimensional array of the MFG task of the 3D human portrait printing product, as shown in Fig. 9.

### 3) THE OTHER ELEMENTS OF NETWORK FORMATION

A complex network also involves directions, edge weights and other elements. In the business process decomposition of MFG tasks, the C3DPO tasks are decomposed layer by layer, and the work content and scope of each layer are determined.

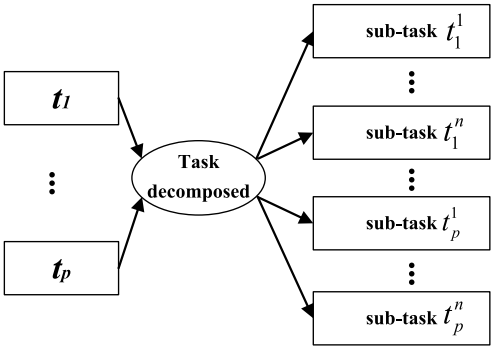


**FIGURE 9.** The *T_Net* model diagram.

However, there are dependency relationships among nodes in the network and in each layer. Therefore, the complex network model of the C3DPOT is a directed network graph.

## C. THE MODEL OF THE C3DPOT NETWORK

The purpose of the digital description of a C3DPOT is mainly to search and match MFG tasks and printing services. Therefore, the specific information in the MFG task description model should correspond to each part of the C3DPS description model. In view of this, the modeling-oriented MFG task description is extended as follows: Taking a user-submitted MFG task as an example, the MFG task is decomposed into several 3D printing order subtasks $t_p$, $p = (1, 2, \ldots, c)$, where $c$ is the number of subtasks, and each subtask $T_p$ can be decomposed according to its task type, also called $t_p^i$, that is, the i-th type of MFG task $p$, $i = (1, 2, \ldots, n)$, where there are $n$ types of MFG tasks. The C3DPOT decomposition diagram is shown in Fig. 10.

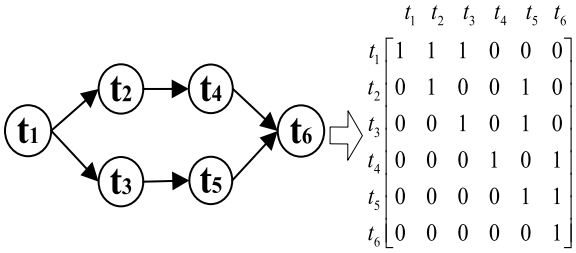


**FIGURE 10.** The C3DPOT decomposition structure diagram.

However, this decomposition structure can be regarded as a subtask with close dependencies, which is closely related to many different levels. Therefore, there is an inheritance relationship between the upper and lower task nodes; that is, subtasks are composed of several tasks at the next level. Then, the "task-to-task" network model is expressed as:

$$\begin{aligned} G_{t-t} &= \{\langle T_{t-t}^1, E_{t-t}^1\rangle, \langle T_{t-t}^2, E_{t-t}^2\rangle, \ldots, \langle T_{t-t}^i, E_{t-t}^i\rangle, \ldots, \\ &\quad \langle T_{t-t}^m, E_{t-t}^m\rangle\} \\ &= \{G_{t-t}^1, G_{t-t}^2, \ldots, G_{t-t}^m\} \end{aligned} \tag{20}$$

where $G_{t-t}$ represents a C3DPOT network with weighted and directed edges and a number of subtasks: $T = \{t_1, t_2, \ldots, t_n\}$; $E^i_{t-t}$ is a task-to-task edge of the C3DPOT network model.

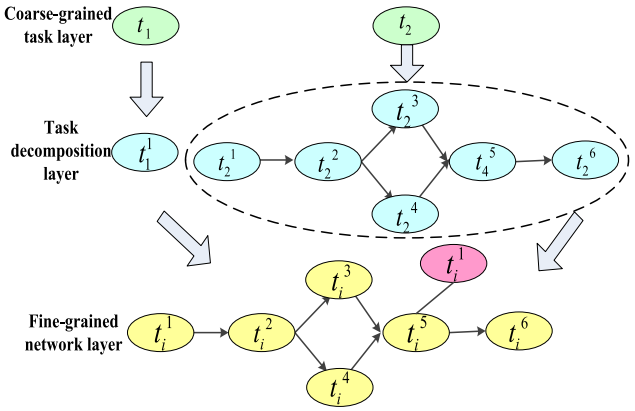


**FIGURE 11.** The C3DPOT network (*T_Net*) structure diagram.

As shown in Fig. 11, *T_Net* is a large virtual network topological structure $G_{t-t}$ that is composed of many MFG task nodes and various related edges [6], [43]. Therefore, a large virtual network topological structure $G_{t-t}$ is composed of several subgraphs, namely,

$$G_{t-t} = \{G^1_{t-t}, G^2_{t-t}, \ldots, G^m_{t-t}\}, \tag{21}$$

where subgraph $G^i_{t-t}$ is composed of several task node sets $T^i_{t-t}$ and edge sets $E^i_{t-t}$ in the C3DPOT, and $1 \le i \le m$.

The binary group expression of the subgraph $G^i_{t-t}$ is

$$G^i_{t-t} = \langle T^i_{t-t}, E^i_{t-t} \rangle, \tag{22}$$

where $T^i_{t-t} = \{t^1_i, t^2_i, \ldots, t^{m_i}_i\}$ refers to the node set of C3DPOT, all nodes $t_i$ have the input attribute and output attribute of the node set, $m_i$ is the decomposed number of complex task nodes, and $E^i_{t-t}$ refers to the mapping relation of the C3DPOT network.

Since an edge between nodes represents the relationship that these nodes are connected in *T_Net*, the corresponding edge set is:

$$E^i_{t-t} = \{e^k_{t-t}\}, \tag{23}$$

where $k = 1, 2, \ldots, m_i$.

Therefore, we have the following analyses from a fine-grained perspective:

(1) If the MFG task $t_p$ is an atomic task, then $m_i = 1$, $t^i_p = \{t^1_i\}$ and $E^i = \phi$. Node $t^1_i$ is also an isolated task node.

(2) If $t_p$ is a complex task, $G^i_{t-t}$ has the following characteristic: The order task has an out-degree, and the degree of the subtask node has an out-degree and in-degree in the *T_Net* network. Therefore, a complex task has only one terminal node, and the C3DPOT network has the following rules:

1) If $e^{k,l}_i = 0$, then there is no direct correlation between atomic task $t^k_i$ and atomic task $t^l_i$;
2) If $e^{k,l}_i = 1$, then there is a direct correlation from atomic task $t^k_i$ to atomic task $t^l_i$;
3) If $e^{k,l}_i = -1$, then there is a direct correlation from atomic task $t^l_i$ to atomic task $t^k_i$.

## IV. CASE STUDY

Taking 3D portrait printing as an example, the user-submitted MFG task is divided into six subtasks by the service demand decomposition module: portrait scanning, cartoon image design and modeling, Model Slicer, 3D printing, surface post-processing and coloring. Fig. 12 shows a diagram of the different mapping mechanisms between service nodes and task nodes.

*The function of mapping mechanisms between service nodes and task nodes is:*

- *Searching and matching independent similar or different functional tasks;*
- *Searching and matching interrelated similar or different functional tasks (service composition);*
- *Providing an evaluation index system for comprehensive utility;*
- *Modeling the evaluation index and utility;*
- *Providing mapping methods for different scheduling problems;*
- *Projecting at the user level based on the mapping between the service and task networks;*
- *Constructing the T_S_Network;*
- *Having a service invocation orientation;*
- …

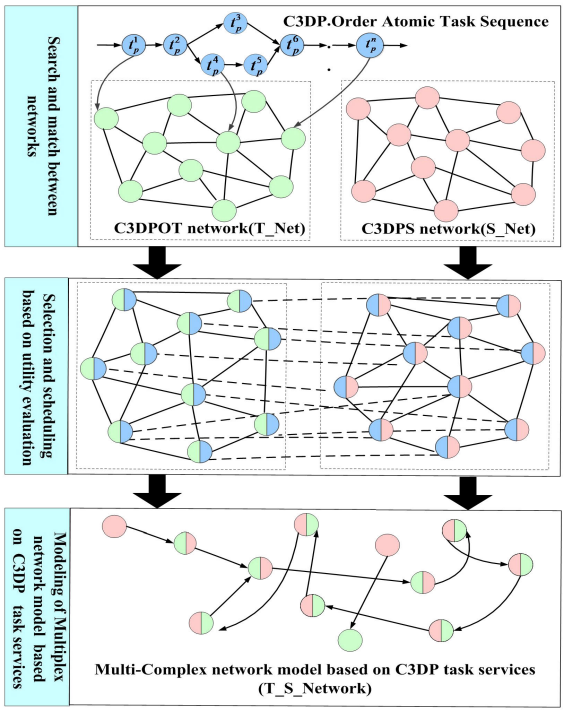


**FIGURE 12.** The different mapping mechanisms between service nodes and task nodes.

Each subtask (such as BMP-A, BMP-B, BMP-C, BMP-D, BMP-E, and BMP-F) corresponds to one of a set of candidate C3DPSs: $WS_1$, $WS_2$, $WS_3$, $WS_4$, $WS_5$ and $WS_6$. Fig. 13 shows a schematic diagram of the relationships between C3DPOTs and C3DPSs.

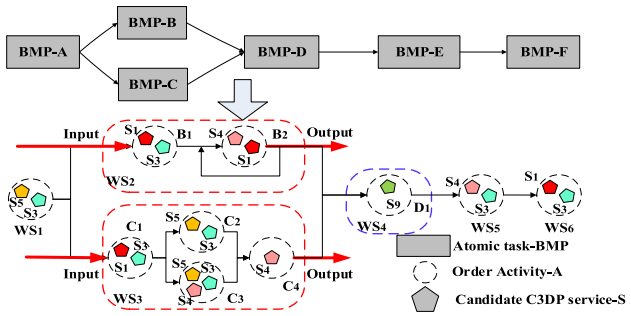


**FIGURE 13.** Schematic diagram of the relationships between C3DPSs and C3DPOTs.

BMP-B is composed of different business logic modules according to the cartoon image design and cartoon image modeling activities. The BMP-B logical relationship between two business logics is concatenation and looping, and the constraint condition is that the two steps have a sequential relationship; BMP-C is composed of multiple subtasks, and the constraint condition is sequential and parallel.

### A. THE MODELING PROCESS OF THE C3DP ORDER TASK NETWORK

Taking the construction of the C3DPOT network as an example, it is used for clustering by the computer program. The basic data of the network is described as a graph in the form of database tables, and then the database table determines the structure of the C3DPOT network. Since the task-service network is a directed logical network, the adjacency matrix is convenient for computer processing, and it is not convenient for expressing the logical network. Therefore, the C3DPOT network topology is expressed as a triple so that the construction process of the network is divided into the following steps:

First, the information of the C3DPOT is expressed.

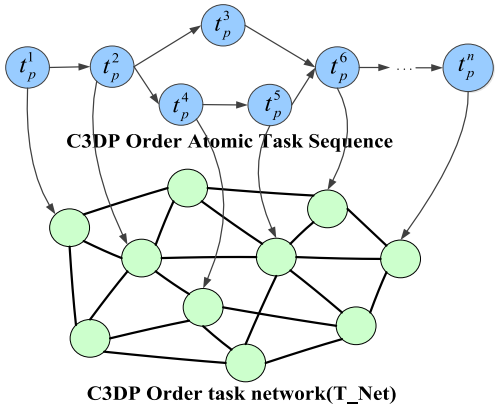


**FIGURE 14.** The relationships of the C3DPOT network.

According to the characteristics of the types and different capabilities, the C3DPOT template is expressed in XML format to assemble resources for personalized design products. For example, some attributes of the No. 6 Yourui 3D Printing studio include C3DPOT Mode, 3D Printing Specification Size, Printing Accuracy, Maximum Printing Speed, 3D Printing Device Model, Printing Type, etc. In Fig. 14, the relationships of the C3DPOT are represented in the description diagram.

Second, the C3DPOT nodes are identified. Here, ten C3DPOTs are selected as the research objects. The C3DPOT network is clustered by the program in the software.

Therefore, the triple data of the cultural creative personalized design products are described as a graph in the form of database tables, and they are used to construct the complex network topology structure. The basic information and data attributes of the C3DPOT nodes are shown in Fig.15.

| ID | NAME | CATEGORY | COMMUNITY | STATUS | REMARK |
|---|---|---|---|---|---|
| 1 | Jiayi Hi-Tech 3D scanner | Portrait scan | 1 | N | (Null) |
| 2 | Yourui 3D scanner | Portrait scan | 2 | N | (Null) |
| 3 | Jiaxuan Three-dimensional design | Cartoon image design | 3 | N | (Null) |
| 4 | XiongzhijiaDesign Center | Cartoon image design and modeling | 4 | N | (Null) |
| 5 | WUT Campus Store | FDM portrait 3D printing | 5 | N | (Null) |
| 6 | Cloud Printing Center | Cloring | 6 | N | (Null) |
| 7 | ..... | ..... | ..... | ..... | ..... |

**FIGURE 15.** The basic information and data attributes of the C3DPOT nodes.

Third, we determine the substitutable relationship between C3DPOT executors and C3DP service providers (that is, the C3DPOT executors can execute the task nodes of competitive relationships). On this basis, the substitutable relationship is created in the table of relational connections.

Random number generators are used to generate the attribute values of the task nodes provided by the resource nodes, as well as the resource names (the indicated positive integers 1, 2, 3…). Then, the resource name is used to determine whether there is a resource allocation relationship between the two nodes. On the basis of the existence of this relationship, the matching degree of resource attribute values is determined to select a better resource allocation relationship as table 2.

Fig. 16 shows the exploded view of the modeling process of the C3DPOT network under the condition of 10 service nodes and 10 task nodes. For both $S\_Net$ and $T\_Net$, if the element of adjacency matrices $e_i^{k,l} = -1$, then there is a blue edge between service nodes $S_i$ and $S_j$ or task nodes ti and tj, which represents a similar-function or similar-demand correlation. However, $e_i^{k,l} = 1$ results in a green edge between service nodes $S_i$ and $S_j$ or task nodes $t_i^l$ and $t_i^k$, which represents a complementary-function or composable-demand correlation. In particular, for the directed network $T\_Net$, a green edge is still directed and determined by the weight $w_{ij} = -1$. If $w_{ij} = 1$, the task node ti is the source node and $t_j$ is the terminal node. Otherwise, $w_{ij} = -1$ means that the edge is directed from $t_i^k$ to $t_i^l$. Moreover, when $e_i^{k,l} = -1$ and $w_{ij} = 0$, there are conflicts in the time constraints so that there is no edge between these two task nodes, even if

| $e_{ij}^{S}$ | $S_1$ | $S_2$ | $S_3$ | $S_4$ | $S_5$ | $S_6$ | $S_7$ | $S_8$ | $S_9$ | $S_{10}$ |
|---|---|---|---|---|---|---|---|---|---|---|
| $S_1$ | 0 | 1 | 0 | 0 | 1 | 0 | 0 | 0 | 0 | 0 |
| $S_2$ | 1 | 0 | 1 | 1 | 1 | 1 | 1 | 1 | 1 | 0 |
| $S_3$ | 0 | 1 | 0 | -1 | 0 | 1 | 1 | 1 | 1 | 1 |
| $S_4$ | 0 | 1 | -1 | 0 | 0 | 1 | 1 | 1 | 1 | 1 |
| $S_5$ | 1 | 1 | 0 | 0 | 0 | 1 | 1 | 1 | 1 | 1 |
| $S_6$ | 0 | 1 | 1 | 1 | 1 | 0 | -1 | -1 | -1 | 1 |
| $S_7$ | 0 | 1 | 1 | 1 | 1 | -1 | 0 | -1 | -1 | 1 |
| $S_8$ | 0 | 1 | 1 | 1 | 1 | -1 | -1 | 0 | -1 | 1 |
| $S_9$ | 0 | 1 | 1 | 1 | 1 | -1 | -1 | -1 | 0 | 1 |
| $S_{10}$ | 0 | 0 | 1 | 1 | 1 | 1 | 1 | 1 | 1 | 0 |

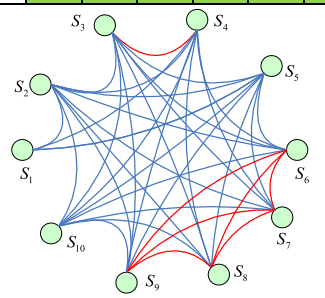


(a) The model of $S\_Net$ based on the adjacency matrix $e_{ij}^{S}$

| $e_{ij}^{k,l}$ / $w_{ij}^{T}$ | | $G_1$ | $G_2$ | | $G_3$ | $G_4$ | | | $G_5$ | | |
|---|---|---|---|---|---|---|---|---|---|---|---|
| | | $t_1$ | $t_2$ | $t_3$ | $t_4$ | $t_5$ | $t_6$ | $t_7$ | $t_8$ | $t_9$ | $t_{10}$ |
| $G_1$ | $t_1$ | 0 | 0 | 0 | 1/0 | 0 | 0 | 0 | 0 | 1/0 | 1/1 |
| $G_2$ | $t_2$ | 0 | 0 | 1/-1 | 1/0 | 1/-1 | 1/0 | 1/0 | 1/0 | 1/-1 | 0 |
| | $t_3$ | 0 | 1/1 | 0 | 0 | 1/0 | -1 | -1 | -1 | 1/0 | 1/0 |
| $G_3$ | $t_4$ | 1/0 | 1/0 | 0 | 0 | 1/-1 | 0 | 0 | 0 | 1/-1 | 0 |
| $G_4$ | $t_5$ | 0 | 1/1 | 1/0 | 1/1 | 0 | 1/0 | 1/-1 | 1/0 | 0 | 0 |
| | $t_6$ | 0 | 1/0 | -1 | 0 | 1/0 | 0 | 1/-1 | -1 | 1/-1 | 1/0 |
| | $t_7$ | 0 | 1/0 | -1 | 0 | 1/1 | 1/1 | 0 | -1 | 1/0 | 1/1 |
| $G_5$ | $t_8$ | 0 | 1/0 | -1 | 0 | 1/0 | -1 | -1 | 0 | 1/1 | 1/1 |
| | $t_9$ | 1/0 | 1/1 | 1/0 | 1/1 | 0 | 1/0 | 1/0 | 1/-1 | 0 | 1/1 |
| | $t_{10}$ | 1/-1 | 0 | 1/0 | 0 | 0 | 1/-1 | 1/-1 | 1/-1 | 1/-1 | 0 |

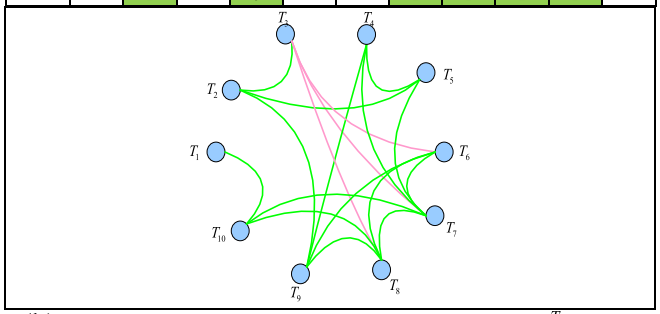


(b) The model of $T\_Net$ based on the adjacency matrix $e_{ij}^{T}$

| $e_{ij}^{S\_T}$ | $S_1$ | $S_2$ | $S_3$ | $S_4$ | $S_5$ | $S_6$ | $S_7$ | $S_8$ | $S_9$ | $S_{10}$ |
|---|---|---|---|---|---|---|---|---|---|---|
| $t_1$ | 0 | 0 | 0 | 0 | 0 | 0 | 0 | 0 | 0 | 1 |
| $t_2$ | 0 | 0 | 0 | 0 | 0 | 0 | 0 | 0 | 1 | 0 |
| $t_3$ | 0 | 0 | 0 | 1 | 0 | 0 | 0 | 0 | 0 | 0 |
| $t_4$ | 0 | 0 | 0 | 1 | 0 | 0 | 0 | 0 | 0 | 0 |
| $t_5$ | 0 | 0 | 1 | 0 | 0 | 1 | 1 | 1 | 0 | 0 |
| $t_6$ | 0 | 1 | 0 | 0 | 0 | 0 | 0 | 0 | 0 | 0 |
| $t_7$ | 0 | 1 | 0 | 0 | 0 | 0 | 0 | 0 | 0 | 0 |
| $t_8$ | 0 | 1 | 0 | 0 | 0 | 0 | 0 | 0 | 0 | 0 |
| $t_9$ | 0 | 1 | 0 | 0 | 0 | 0 | 0 | 0 | 0 | 0 |
| $t_{10}$ | 0 | 0 | 0 | 1 | 0 | 0 | 0 | 0 | 0 | 0 |

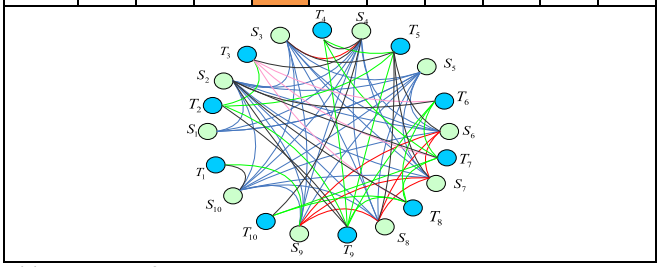

(c) The model of $Matching\_Net$ based on the adjacency matrix $E_{ij}^{S\_T}$

**FIGURE 16.** The model of the supply-demand network of C3DP.

**TABLE 2.** the data attributes of C3DPOT nodes.

| Row-Key | Time-Stamp | Columns | | | |
|---|---|---|---|---|---|
| | | ORNAME | ORCATE-GORY | PRTECHNOLOGY | PRMATERIAL |
| 00001 | 0 | bas Brahma decor plaster | 1 | Plaster 3D printing (PP) | Plaster materials |
| 00002 | 0 | R2D2 robot | 3 | Selective laser sintering (SLS) | Mineral powder |
| 00003 | 1 | Hole cube model | 1 | Stereo lithography apparatus (SLA) | Photo polymer |
| 00004 | 0 | Eiffel Tower | 7 | Fused deposition modeling (FDM) | Thermoplastic materials |

their functions are complementary. In addition, similar to the bipartite graph, there exists a red edge implying matchable correlations between service node $S_i$ and task node $t_j$. Clearly, the adjacency matrices $e_{ij}^S$ and $e_{ij}^T$ are symmetric matrices, and $W^T$ is an anti-symmetric matrix.

Similarly, according to the above method and steps, two more simulations with different node expansions are carried out. Fig. 17 shows the simulation results, in a circular layout and in a random layout, of different modeled complex networks (i.e., (a) has 10 services and 10 task nodes in a C3DP supply-demand network, (b) has 20 services and 20 task nodes in a C3DP supply-demand network, and (c) has 10 services and 10 task nodes in a C3DP supply-demand network.

Finally, the basic information table and connectional relationship table data of the C3DP service nodes are imported and analyzed in the Gephi-0.8.1 software. As shown in Fig. 18, the topology of the C3DP service network is composed of 33 nodes and 46 edges.

If the colors of nodes are the same, this indicates that their C3DP services are similar. The thickness of an edge represents the similarity between two C3DPSs; that is, there are many alternative relationships between service capabilities.

Similar reasoning, there is a large correlation between two C3DPSs nodes and these nodes are clustered. The matching degree between these two nodes is greater than the others, and the matching relationship between the nodes.

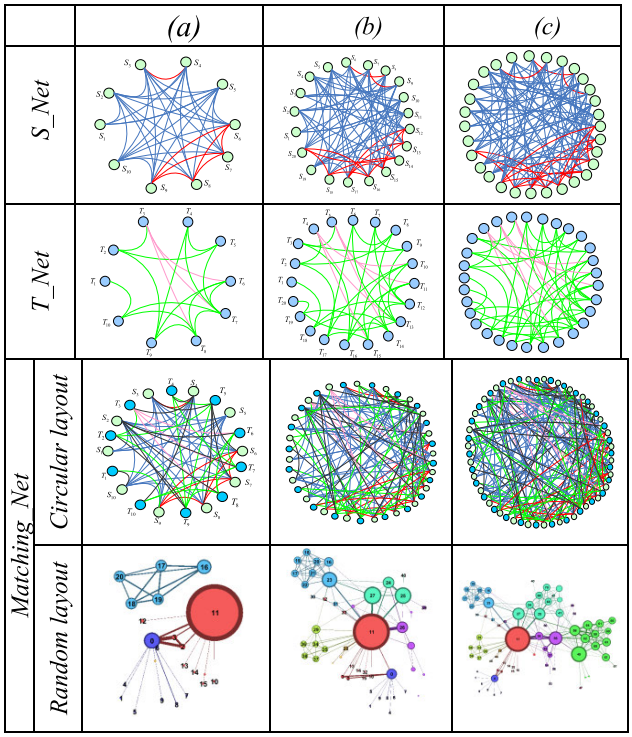


(a) 10 services and 10 task nodes

(b) 20 services and 20 task nodes

(c) 30 services and 30 task nodes

**FIGURE 17.** under different C3DP networks.

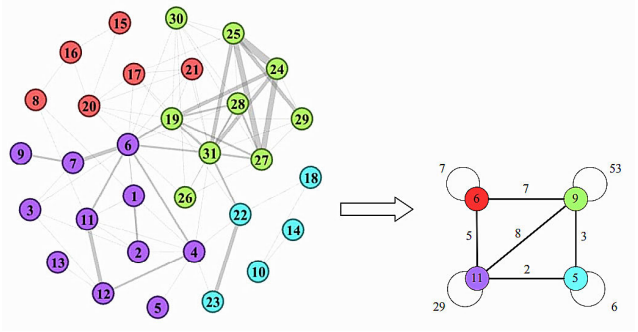

**FIGURE 18.** The node diagram of a C3DP service network.

### *B. THE SIMULATION OF THE C3DP ORDER TASK NETWORK*

In the CMfg mode, it is necessary for the model to accord with certain rules and to self-organize to achieve the efficient operation and management of MFG services. It is important to enable the distribution and use of CMfg services on demand. On the basis of the shortcomings of the existing modeling of MFG services, this paper proposes a modeling and clustering analysis method based on complex network theory.

At present, MFG service modeling research focuses on the service description of resource discovery matching. The purpose of this research is to establish a service-oriented description model that easily directly matches the MFG task requirements and demand-side MFG and then delivers the results. On the basis of a detailed analysis of each matching index, the matching index's data sets are simulated with the traditional MFG service modeling method and 11 kinds of similarity algorithms based on complex networks. All the algorithms' code is written on the MATLAB experimental platform, with a Windows 7 operating system and an Intel i3-2120 (3.30 GHz) CPU with 4 G memory [6], [43]. In the experiments, 90% of five data sets were selected as training sets and 10% as test sets, and the number of independent experiments was 1000. The resulting accuracy AUC values of the traditional MFG service modeling method and 11 kinds of

**TABLE 3.** The resulting accuracy AUC values (%) of the traditional method and 11 kinds of similarity algorithms based on complex networks.

| Types | The traditional method | | | 11 kinds of similarity algorithms based on complex networks | | | | |
|---|---|---|---|---|---|---|---|---|
| | Exact matching | Compatible matching | Contains matching | USAir | NS | Grid | Yeast | PB |
| HPI | 3.561 | 2.654 | 1.201 | 0.051 | 0.967 | 9.534 | 2.425 | 0.870 |
| CN | 2.995 | 1.325 | 1.235 | 0.062 | 0.267 | 2.481 | 0.701 | 0.375 |
| PA | 3.056 | 1.254 | 1.204 | 0.031 | 0.735 | 7.992 | 1.684 | 0.523 |
| AA | 1.854 | 1.025 | 1.054 | 0.048 | 0.450 | 5.161 | 1.186 | 0.469 |
| RA | 2.056 | 2.985 | 1.069 | 0.028 | 0.365 | 3.114 | 0.891 | 0.443 |
| CI | 1.952 | 1.985 | 1.211 | 0.034 | 0.384 | 3.150 | 0.931 | 0.590 |

**TABLE 4.** the operating time (s) of the traditional method and 11 kinds of similarity algorithms based on complex networks.

| Types | The traditional method | | | 11 kinds of similarity algorithms based on complex networks | | | | |
|---|---|---|---|---|---|---|---|---|
| | Exact matching | Contains matching | Contains matching | USAir | NS | Grid | Yeast | PB |
| HPI | 5.6540 | 4.5681 | 3.9854 | 7.4501 | 0.5019 | 0.1542 | 0.1812 | 0.4106 |
| CN | 4.8956 | 4.2658 | 3.6857 | 7.2822 | 1.8441 | 0.0519 | 0.5931 | 1.1370 |
| PA | 5.6985 | 5.3654 | 4.9887 | 13.281 | 0.3361 | 0.0142 | 0.1586 | 0.8125 |
| AA | 2.6542 | 2.3658 | 1.5874 | 8.5460 | 1.0824 | 0.0245 | 0.3540 | 0.9125 |
| RA | 3.6521 | 3.0554 | 2.3652 | 16.642 | 1.3254 | 0.4089 | 0.4752 | 0.9524 |
| CI | 6.8755 | 4.5697 | 3.6858 | 13.542 | 1.2843 | 0.0451 | 0.4525 | 0.7158 |

similarity algorithms based on complex networks are shown in Table 3:

The relationships between the maximum link ratio and the ratio of deleted nodes is shown in Fig. 19 (a) and (b).

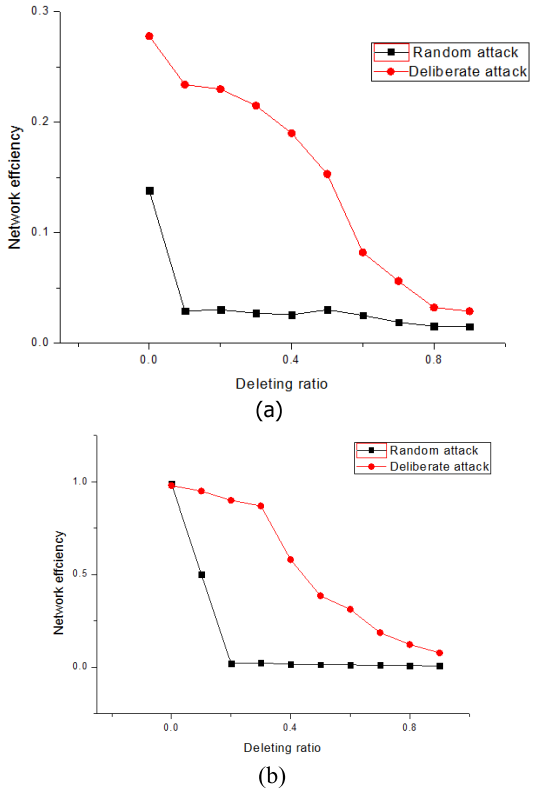


**FIGURE 19.** The relationship between the maximum link ratio and the ratio of deleted nodes.

By comparing and analyzing the experimental results of Table 3 and Fig. 19, it is shown that the combined index (CI) algorithm is more accurate than the traditional method and the existing 11 algorithms in five different domain networks, which further improves the accuracy of link prediction and has better prediction results for complex networks; that is, the applicability of the CI algorithm is more universal than that of the other algorithms. Additionally, a visualization of the NS network is shown in Fig. 20. The five indicators other than the PA indicator have the highest AUC value, which may be related to the large module degree due to the comparison of the traditional method and 11 kinds of similarity algorithms based on complex networks. Considering the theoretical time complexity of the algorithms, the common neighbor algorithm first finds a pair of nodes and then calculates the number of common neighbors. Therefore, the time complexity of the algorithm is 220 (k N). On this basis, the AA and RA indicators are calculated for neighbors.

Therefore, the C3DPS network modeling method maintains the same time complexity as the traditional modeling method, and its accuracy is improved. Here, the running time of the algorithm is also tested. As shown in Table 4, the actual elapsed time of CI is relatively short, which shows that the actual efficiency of the algorithm is relatively high.

## V. CONCLUSION

To analyze the characteristics of dynamics and differences in C3DPOTs and C3DPSs, an order-driven C3DP task-service network modeling method is proposed. First, multiplex network models based on C3DP task services are constructed according to the relationships among services, among tasks and between services and tasks. Then, on the basis of the description of a C3DP task and the definition of its constraint structure, C3DP order task network modeling is proposed. Finally, a C3DP T_Net model example is designed to verify the feasibility of the method.

However, the results of applying the optimization solutions for cloud 3D printing task modeling for complex networks and the dynamic evolution and analysis of the complex network model for the improvement and evaluation of supply-demand matching are highlighted by the work on modeling the C3DPOT provided in this paper. Considering the expansion ability of the proposed C3DPOT network model of *T_Net*, the proposed *Matching_Net* is just the fundamental elementary model for functional matching. Further work is needed to improve and enrich the models, and there are also potential directions for supply-demand matching

and optimal allocation. Potential further work includes the following:

(1) For different objectives of different tasks (orders, consumers, and operators) in SOM systems, it is necessary to enrich the network-related attributes of various nodes and edges in the models of $T\_Net$.

(2) For different kinds of tasks and services, by evaluating the quality of manufacturing resources and scheduling problems as well as the uncertainty of user participation and the dynamics of the implementation process, there is room for a series of works on optimization with the corresponding objective functions, constraints and algorithms based on the proposed C3DPOT network model of $T\_Net$.

(3) Rather than performing static matching or mapping in the proposed $T\_Net$, further analysis of how the models of $T\_Net$ evolve dynamically with time is also significant and urgently needs to be addressed.

## REFERENCES


[1] Y. B. Seo, Y. H. Yun, and K.-N. Joo, "3D multi-layered film thickness profile measurements based on photometric type imaging ellipsometry," *Int. J. Precis. Eng. Manuf.*, vol. 17, no. 8, pp. 989–993, Aug. 2016.

[2] S. L. Jung, Y.-J. Seol, M. Sung, W. Moon, S. W. Kim, J.-H. Oh, and D.-W. Cho, "Development and analysis of three-dimensional, 3D printed biomimetic ceramic," *Int. J. Precis. Eng. Manuf.*, vol. 17, no. 12, pp. 1711–1719, 2016.

[3] S. Kim, J. Lee, and B. Choi, "3D printed fluidic valves for remote operation via external magnetic field," *Int. J. Precis. Eng. Manuf.*, vol. 17, no. 7, pp. 937–942, Jul. 2016.

[4] Y. Zhuang, "Research of information exchange module and knowledge service system based on the cloud manufacturing service platform," Ph.D. dissertation, Dept. Comput., Inner Mongolia Univ. Sci. Technol., Baotou City, MA, USA, 2014.

[5] G. Guerrero, J. A. Langa, and A. Suárez, "Architecture of attractor determines dynamics on mutualistic complex networks," *Nonlinear Anal. Real World Appl.*, vol. 34, pp. 17–40, Apr. 2017.

[6] Y. Cheng, F. Tao, L. Zhang, and D. Zhao, "Dynamic supply-demand matching for manufacturing resource services in service-oriented manufacturing systems: A hypernetwork-based solution framework," in *Proc. Int. Manuf. Sci. Eng. Conf. (ASME)*, 2015, vol. 7, no. 429, Art. no. V002T04A017-1.

[7] F. Tao, J. Cheng, Y. Cheng, S. Gu, T. Zheng, and H. Yang, "SDMSim: A manufacturing service supply–demand matching simulator under cloud environment," *Robot. Comput.-Integr. Manuf.*, vol. 45, pp. 34–46, Jun. 2017.

[8] Y. Cheng, F. Tao, L. Xu, and D. Zhao, "Advanced manufacturing systems: Supply–demand matching of manufacturing resource based on complex networks and Internet of Things," *Enterprise Inf. Syst.*, vol. 2016, pp. 1–18, 2016.

[9] W. J. Feng, C. Yin, X.-B. Li, and L. Li, "A classification matching method for manufacturing resource in cloud manufacturing environment," *Int. J. Model. Simul. Sci. Comput.*, vol. 08, no. 2, pp. 58–72, 2017.

[10] Y. Cheng, F. Tao, D. Zhao, and L. Zhang, "Modeling of manufacturing service supply–demand matching hypernetwork in service-oriented manufacturing systems," *Robot. Comput.-Integr. Manuf.*, vol. 45, pp. 59–72, Jun. 2017.

[11] M. R. Raman, N. Somu, K. Kirthivasan, and V. S. S. Sriram, "A hyper graph and arithmetic residue-based probabilistic neural network for classification in intrusion detection systems," *Neural Netw.*, vol. 92, pp. 52–64, Aug. 2017.

[12] J.-H. Kim and H.-Y. Song, "Hypergraph-based binary locally repairable codes with availability," *IEEE Commun. Lett.*, vol. 21, no. 11, pp. 2332–2335, Nov. 2017.

[13] C. L. Zhang, B. Sheng, X. Yin, F. Zhao, and Y. Shu, "Research and development of off-line services for the 3D automatic printing machine based on cloud manufacturing," *J. Ambient Intell. Humanized Comput.*, no. 1, pp. 1–20, 2017.

[14] J. Minguella, M. Villegas, B. Poll, G. Tena, J. A. Calero, M. P. Ginebra, and F. Korkusuz, "Automatic casting of advanced technical ceramic parts via open source high resolution 3D printing machines," *Key Eng. Mater.*, vol. 631, pp. 269–274, Nov. 2014.

[15] S. Im, Y. Lee, J. Kim, and M. Chang, "A solution for camera occlusion using a repaired pattern from a projector," *Int. J. Precis. Eng. Manuf.*, vol. 17, no. 11, pp. 1443–1450, Nov. 2016.

[16] Y. Yasami, "A new knowledge-based link recommendation approach using a non-parametric multilayer model of dynamic complex networks," *Knowl.-Based Syst.*, vol. 143, pp. 81–92, Mar. 2018.

[17] Y. Yasami and F. Safaei, "A statistical infinite feature cascade-based approach to anomaly detection for dynamic social networks," *Comput. Commun.*, vol. 100, pp. 52–64, Mar. 2017.

[18] F. Tao, L. Zhang, K. Lu, and D. Zhao, "Study on manufacturing grid resource service optimal-selection and composition framework," *Enterprise Inf. Syst.*, vol. 6, no. 2, pp. 237–264, 2012.

[19] F. Tao, C. Li, T. W. Liao, and Y. J. Laili, "BGM-BLA: A new algorithm for dynamic migration of virtual machines in cloud computing," *IEEE Trans. Services Comput.*, vol. 9, no. 6, pp. 910–925, Nov./Dec. 2016.

[20] Z. Wen, X. Liu, and Y. Xu, "A RESTful framework for Internet of Things based on software defined network in modern manufacturing," *Int. J. Adv. Manuf. Technol.*, vol. 84, nos. 1–4, pp. 1–9, 2016.

[21] T. X. Song, C. L. Zhang, and B. Q. Huang, "A cloud manufacturing service platform for small and medium enterprises," *Comput. Integr. Manuf. Syst.*, vol. 5, no. 5, pp. 47–52, 2013.

[22] D. Wu, D. W. Rosen, L. Wang, and D. Schaefer, "Cloud-based design and manufacturing: A new paradigm in digital manufacturing and design innovation," *Comput.-Aided Des.*, vol. 59, pp. 1–14, Feb. 2015.

[23] X. W. Liu, Y. Yang, X. D. Xu, C. C. Li, and L. P. Ran, "Research on profit mechanism of 3D printing cloud platform based on customized products," *Appl. Mech. Mater.*, vol. 703, pp. 318–322, Dec. 2014.

[24] C.-M. Wei, C.-L. Zhang, T.-X. Song, and B.-Q. Huang, "A cloud manufacturing service management model and its implementation," in *Proc. Int. Conf. Service Sci. (ICSS)*, Apr. 2013, pp. 60–63.

[25] N. M. Ahmed and L. Chen, "An efficient algorithm for link prediction in temporal uncertain social networks," *Inf. Sci.*, vol. 331, pp. 120–136, Feb. 2016.

[26] Z. Chen, W. Hendrix, and N. F. Samatova, "Community-based anomaly detection in evolutionary networks," *Inf. Syst*, vol. 5, 39, No, pp. 85–159, 2012.

[27] H. Fanaee-T and J. Gama, "Tensor-based anomaly detection: An interdisciplinary survey," *Knowl.-Based Syst.*, vol. 98, pp. 130–147, Apr. 2016.

[28] Y. Chen, D. Miao, and H. Zhang, "Neighborhood outlier detection," *Expert Syst. Appl.*, vol. 37, no. 12, pp. 8745–8749, Dec. 2010.

[29] N. A. Heard, D. J. Weston, K. Platanioti, and D. J. Hand, "Bayesian anomaly detection methods for social networks," *Ann. Appl. Statist.*, vol. 4, no. 2, pp. 645–662, Jun. 2010.

[30] D. Wu, J. L. Thames, D. W. Rosen, and D. Schaefer, "Enhancing the product realization process with cloud-based design and manufacturing systems," *J. Comput. Inf. Sci. Eng.*, vol. 13, no. 4, pp. 1172–1186, Dec. 2013.

[31] H. Anwar, I. Din, and K. Park, "Projector calibration for 3D scanning using virtual target images," *Int. J. Precis. Eng. Manuf.*, vol. 13, no. 1, pp. 125–131, Jan. 2012.

[32] C. Yin, Q. Xia, and Z. W. Li, "Semantic matching technique of cloud manufacturing service based on OWL-S," *Comput. Integr. Manuf. Syst.*, vol. 7, no. 7, pp. 1494–1502, 2012.

[33] Y. Laili, F. Tao, L. Zhang, Y. Cheng, Y. Luo, and B. R. Sarker, "A ranking chaos algorithm for dual scheduling of cloud service and computing resource in private cloud," *Comput. Ind.*, vol. 64, no. 4, pp. 448–463, May 2013.

[34] S. Ding, H. Jia, M. Du, and Y. Xue, "A semi-supervised approximate spectral clustering algorithm based on HMRF model," *Inf. Sci.*, vol. 429, pp. 215–228, Mar. 2018.

[35] Y. Zhang, J. Wen, X. Wang, and Z. Jiang, "Semi-supervised learning combining co-training with active learning," *Expert Syst. Appl.*, vol. 41, no. 5, pp. 2372–2378, Apr. 2014.

[36] M. Fatehi and H. H. Asadi, "Application of semi-supervised fuzzy c-means method in clustering multivariate geochemical data, a case study from the Dalli Cu-Au porphyry deposit in central Iran," *Ore Geol. Rev.*, vol. 81, pp. 245–255, Mar. 2017.
[37] S. Usuki, H. Kanaka, and K. T. Miura, "Generation and control of 3D standing wave illumination for wide-field high-resolution 3D microscopic measurement," *Int. J. Precis. Eng. Manuf.*, vol. 14, no. 1, pp. 55–60, Jan. 2013.
[38] K. Cheng, W. Liu, Y. Xiaohan, Y. Chengxiang, K. Ruizhi, "Improving hierarchical task network planning performance by the use of domain-independent heuristic search," *Knowl.-Based Syst.*, vol. 142, pp. 131–143, Feb. 2018.
[39] K. Janowicz and M. Wilkes, "SIM-DLA: A novel semantic similarity measure for description logics reducing inter-concept to inter-instance similarity," in *Proc. Eur. Semantic Web Conf. Semantic Web Res. Appl.*, 2009, pp. 353–367.
[40] J. Zhou, X. Yao, Y. Lin, F. T. S. Chan, and Y. Li, "An adaptive multi-population differential artificial bee colony algorithm for many-objective service composition in cloud manufacturing," *Inf. Sci.*, vol. 456, pp. 9–16, Aug. 2018.
[41] K. Liu, S. Li, X. Qie, Y. Du, R. Jiang, G. Lu, X. Mou, and G. Liu, "Analysis and investigation on lightning electromagnetic coupling effects of a dipole antenna for a wireless base station," *IEEE Trans. Electromagn. Compat.*, vol. 60, no. 6, pp. 1842–1849, Dec. 2018.
[42] F. T. Azadbakht and G. R. Boroun, "Decoupling of the leading order DGLAP evolution equation with spin dependent structure functions," *Int. J. Theor. Phys.*, vol. 57, no. 2, pp. 1–11, 2018.
[43] Y. Cheng, D. Zhao, F. Tao, L. Zhang, and Y. Liu, "Complex networks based manufacturing service and task management in cloud environment," in *Proc. IEEE Ind. Electron. Appl.*, Jun. 2015, pp. 242–247.